

## Supporting Information

### Computational design of a notable nitrogen-rich energetic compound on the basis of Diels-Alder reaction

Junqing Yang<sup>ab\*</sup>, Gazi Hao<sup>c</sup>, Rui Guo<sup>a</sup>, Hu Guo<sup>c</sup>, Wei Jiang<sup>c</sup>, Jianguo Zhang<sup>b\*</sup>

<sup>a</sup> School of Mechanical Engineering, Nanjing University of Science and Technology, Nanjing, 210094, China

<sup>b</sup> State Key Laboratory of Explosion Science and Technology, Beijing Institute of Technology, Beijing, 100081, China

<sup>c</sup> National Special Superfine Powder Engineering Research Center, Nanjing University of Science and Technology, Nanjing, 210094, China.

## Table of Contents

<b>All involved computational details and formulas:</b> .....	S3
<b>Figure S1.</b> Reaction activation Gibbs free energy ( $\Delta G^\ddagger$ , in $\text{kJ}\cdot\text{mol}^{-1}$ ) of each D–A reaction ( <b>Series a-d</b> ). .....	S4
<b>Table S1.</b> $\Delta G^\ddagger_{\text{dist-diene}}$ , $\Delta G^\ddagger_{\text{dist-dienophile}}$ , $\Delta G^\ddagger_{\text{dist}}$ , $\Delta G^\ddagger_{\text{int}}$ , and $\Delta G^\ddagger$ (in $\text{kJ}\cdot\text{mol}^{-1}$ ) of the D–A reactions between ethylene and 17 aromatic dienes, together with the NICS(0) and NICS (1) values (in ppm) of these dienes. ....	S4
<b>Figure S2.</b> Optimized geometries of involving compounds in Reaction process of <b>EC-1</b> .....	S5
<b>Figure S3.</b> Electrostatic potential (ESP) on the 0.001 au molecular surface of <b>EC-1</b> . .....	S5
<b>Figure S4.</b> The area percent in electrostatic potential range of <b>EC-1</b> .....	S5
<b>Figure S5.</b> Possible pyrolysis processes for <b>EC-1</b> , together with the $\Delta E_{\text{BD}}$ and $\Delta E^\ddagger$ , in $\text{kJ}\cdot\text{mol}^{-1}$ . .....	S6
<b>Figure S6.</b> Energy profile and the optimized geometries of involving compounds during the most possible pyrolysis process ( $\text{N}_2$ elimination process) of <b>EC-1</b> .....	S6
<b>Table S2.</b> $OB$ (%), $\rho$ ( $\text{g}\cdot\text{cm}^{-3}$ ), $\Delta H_f^\circ$ (s) ( $\text{kcal}\cdot\text{mol}^{-1}$ ), $D$ ( $\text{km}\cdot\text{s}^{-1}$ ), $P$ (GPa), $\Delta V$ ( $\text{\AA}^3$ ), and $\rho Q_{\text{max}}$ ( $\text{kcal}\cdot\text{cm}^{-3}$ ) of <b>EC-1</b> , <i>trans</i> - <b>BIT</b> , and <b>RDX</b> . .....	S6
<b>Table S3.</b> Cell parameters predicted with Dreiding force field for <b>EC-1</b> .....	S7
<b>Figure S7.</b> The most possible crystal packing of <b>EC-1</b> predicted by using Dreiding force field. ....	S7
<b>Figure S8.</b> The predicted IR spectrum of <b>EC-1</b> at the M06-2X/6-31G(d) level. ....	S7
<b>Figure S9.</b> The predicted IR spectrum of cyclopentadiene ( <b>0N</b> ) at the M06-2X/6-31G(d) level (up) and its experimental IR spectrum (bottom) .....	S8
<b>The Cartesian coordinates of all involved compounds in the reaction process of EC-1 optimized at the M06-2X/6-31G(d) level.</b> .....	S9
<b>The Cartesian coordinates of all involved compounds in the <math>\text{N}_2</math> elimination process of EC-1 optimized at the M06-2X/6-31G(d) level.</b> .....	S11
References .....	S13

### All involved computational details and formulas:

All geometry optimizations and frequency calculations were performed with DFT method at M06-2X/6-31G(d) and B3PW91/6-31G(d,p) levels by using Gaussian 09 software<sup>1</sup>. Frequency calculations ensure that reactants and products have not any imaginary frequency and the TSs have only one imaginary frequency. The intrinsic reaction coordinate (IRC) analyses confirmed that the TSs truly associate to the minima of the reactants and the products.

The  $\rho$  was predicted by equation (1):<sup>2</sup>

$$\rho = \alpha_1(M/V_m) + \beta_1(\nu\sigma_{\text{tot}}^2) + \gamma_1 \quad (1)$$

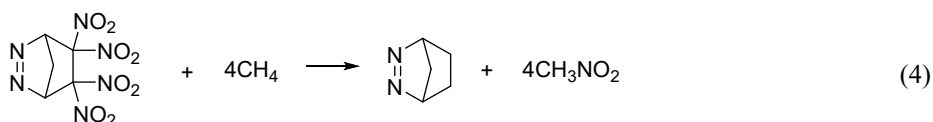
where  $M$  is the molecular weight ( $\text{g}\cdot\text{mol}^{-1}$ );  $V_m$  is the average molar volume within the 0.001 a.u. electron density contour ( $\text{cm}^3\cdot\text{mol}^{-1}$ );  $\nu$  is the degree of balance between positive and negative potential on the molecular surface;  $\sigma_{\text{tot}}^2$  is a measure of variability of the electrostatic potential ( $\text{kcal}^2\cdot\text{mol}^{-2}$ ); The coefficients  $\alpha_1$ ,  $\beta_1$ , and  $\gamma_1$  at the B3PW91/6-31G(d,p) level are 0.9183, 0.0028, and 0.0443, respectively.<sup>2</sup>

The  $\Delta H_f^\circ(\text{s})$  was estimated using the following equations (2-3):<sup>3</sup>

$$\Delta H_f^\circ(\text{s}) = \Delta H_f^\circ(\text{g}) - \Delta H_{\text{sub}} \quad (2)$$

$$\Delta H_{\text{sub}} = \alpha_2 A_S^2 + \beta_2(\nu\sigma_{\text{tot}}^2)^{0.5} + \gamma_2 \quad (3)$$

where  $\Delta H_f^\circ(\text{g})$  is the gas-phase heat of formation which was estimated by designing the following isodesmic reaction (4);  $\Delta H_{\text{sub}}$  is the sublimation enthalpy;  $A_S$  is the area of the isosurface of 0.001 e/Bohr<sup>3</sup> electron density of the molecule ( $\text{\AA}^2$ ); The coefficients  $\alpha_2$ ,  $\beta_2$ , and  $\gamma_2$  at the B3PW91/6-31G(d,p) level are  $4.43 \times 10^{-4}$ , 2.0599, and -2.4825, respectively.<sup>3</sup>



Thermal stability was examined by calculating the bond dissociation energy ( $\Delta E_{\text{BD}}$ ) and the decomposition activation energy barrier ( $\Delta E^\ddagger$ ) of all possible pyrolysis processes. The sensitivity was evaluated by predict the free space in the lattice ( $\Delta V$ )<sup>4, 5</sup> and the maximum heat of detonation per unit volume ( $\rho Q_{\text{max}}$ )<sup>4-6</sup>. The formulas are as follows:

$$\Delta E_{\text{BD}}(\text{A-B}) = E_{\text{A}\cdot} + E_{\text{B}\cdot} - E_{\text{A-B}} \quad (5)$$

$$\Delta E^\ddagger = E_{\text{TS}} - E_{\text{A-B}} \quad (6)$$

$$\Delta V = V_{\text{eff}} - V_{\text{int}} \quad (7)$$

where A-B is the neutral reactant; A· and B· are the corresponding radical products after the dissociation of A-B bond; TS is the transition state in the pyrolysis process;  $E_{\text{A}\cdot}$ ,  $E_{\text{B}\cdot}$ ,  $E_{\text{A-B}}$ , and  $E_{\text{TS}}$  are their corresponding total energies

after the correction of the zero-point energy;  $V_{\text{eff}}$  is the effective volume of the molecule that would correspond to 100% packing of the unit cell, which is usually quite similar to the 0.001 au contour of the molecule's electronic density;  $V_{\text{int}}$  is the space encompassed by the 0.003 au contour of the molecule's electronic density.

The polymorph of **EC-1** was predicted by searching the molecular packings among seven most possible space groups ( $C2/c$ ,  $P2_1$ ,  $P2_1/c$ ,  $P1$ ,  $P2_12_12_1$ ,  $Pbca$ , and  $Pna2_1$ ) by using Dreiding force field<sup>7</sup> and Polymorph module of Materials Studio software<sup>8</sup>. The electrostatic and van der Waals interactions are selected to Ewald and Atom based, respectively.

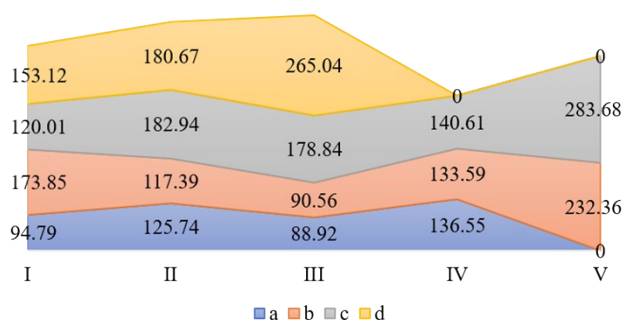


**Figure S1.** Reaction activation Gibbs free energy ( $\Delta G^\ddagger$ , in  $\text{kJ}\cdot\text{mol}^{-1}$ ) of each D–A reaction (**Series a-d**).

**Table S1.**  $\Delta G^\ddagger_{\text{dist-diene}}$ ,  $\Delta G^\ddagger_{\text{dist-dienophile}}$ ,  $\Delta G^\ddagger_{\text{dist}}$ ,  $\Delta G^\ddagger_{\text{int}}$ , and  $\Delta G^\ddagger$  (in  $\text{kJ}\cdot\text{mol}^{-1}$ ) of the D–A reactions between ethylene and 17 aromatic dienes, together with the NICS(0) and NICS (1) values (in ppm) of these dienes.

Dienes	$\Delta G^\ddagger_{\text{dist-diene}}$	$\Delta G^\ddagger_{\text{dist-dienophile}}$	$\Delta G^\ddagger_{\text{dist}}$	$\Delta G^\ddagger_{\text{int}}$	$\Delta G^\ddagger$	NICS(0)	NICS (1)
<b>0N</b>	63.74	25.80	89.54	5.25	94.79	-2.7260	-5.4644
<b>1N-I</b>	87.21	34.35	121.56	4.18	125.74	-2.7869	-6.7577
<b>1N-II</b>	63.32	22.39	85.71	3.20	88.92	-0.8175	-6.2295
<b>1N-III</b>	101.56	51.91	153.47	-16.92	136.55	-15.7534	-11.9220
<b>2N-I</b>	110.02	42.07	152.10	21.76	173.85	-3.1729	-7.9993
<b>2N-II</b>	88.21	30.02	118.23	-0.83	117.39	-1.3625	-7.4592
<b>2N-III</b>	70.93	22.47	93.40	-2.84	90.56	-0.0645	-7.1982
<b>2N-IV</b>	103.69	48.53	152.22	-18.63	133.59	-14.4206	-12.1437
<b>2N-V</b>	165.79	49.19	214.97	17.39	232.36	-15.3908	-13.0016
<b>3N-I</b>	92.51	25.73	118.24	1.76	120.01	-0.5641	-9.1562
<b>3N-II</b>	130.29	56.17	186.46	-3.52	182.94	-14.7492	-14.4732
<b>3N-III</b>	133.68	59.17	192.84	-14.00	178.84	-13.8860	-12.9131
<b>3N-IV</b>	116.96	47.20	164.16	-23.55	140.61	-13.0269	-12.5978
<b>3N-V</b>	210.95	47.84	258.79	24.89	283.68	-15.1184	-14.4956
<b>4N-I</b>	122.25	27.99	150.24	2.88	153.12	-5.0621	-10.5709
<b>4N-II</b>	142.69	54.20	196.89	-16.22	180.67	-14.1547	-14.8677

4N-III	198.73	46.12	244.84	20.20	265.04	-14.5034	-15.2727
--------	--------	-------	--------	-------	--------	----------	----------

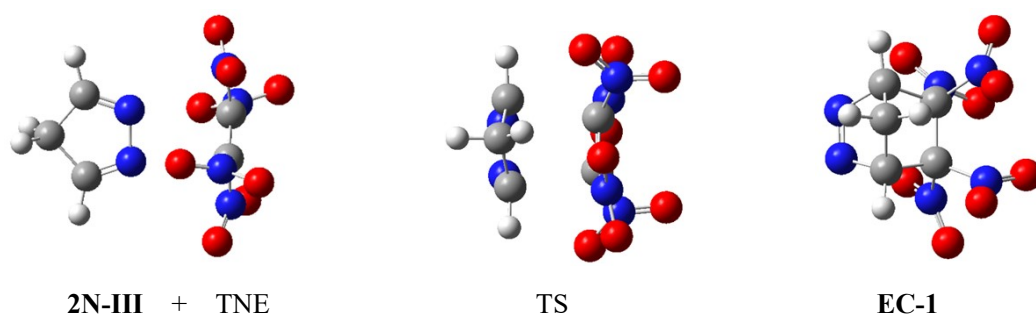


Figure S2. Optimized geometries of involving compounds in Reaction process of EC-1

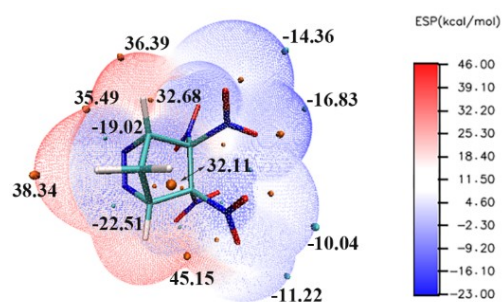


Figure S3. Electrostatic potential (ESP) on the 0.001 au molecular surface of EC-1 (blue and red points denote the surface local minima and maxima, respectively).

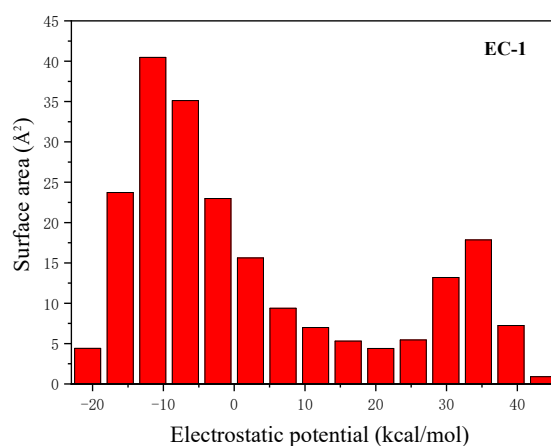
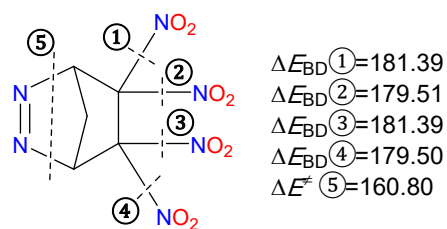
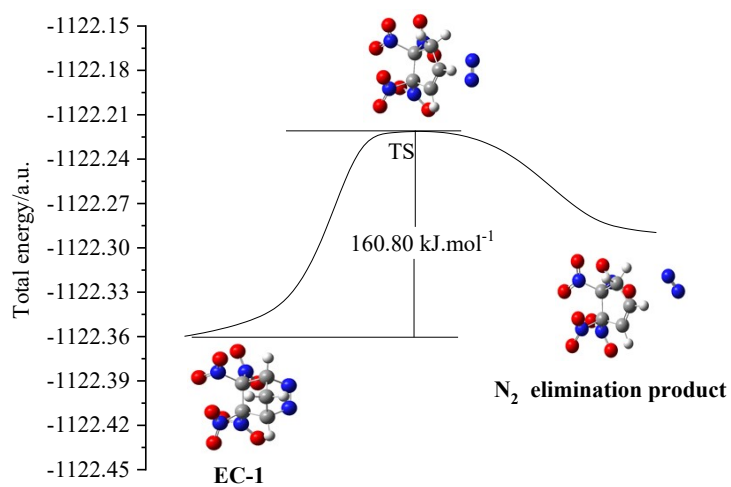


Figure S4. The area percent in electrostatic potential range of EC-1



**Figure S5.** Possible pyrolysis processes for **EC-1**, together with the  $\Delta E_{BD}$  and  $\Delta E^\ddagger$ , in  $\text{kJ}\cdot\text{mol}^{-1}$ .



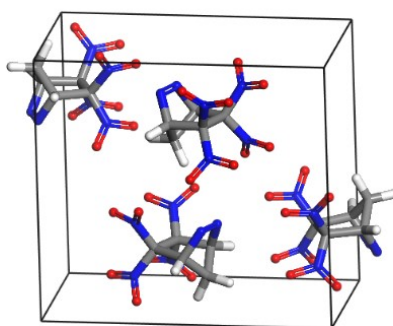
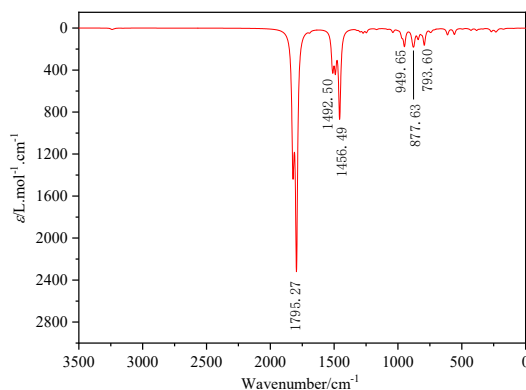
**Figure S6.** Energy profile and the optimized geometries of involving compounds during the most possible pyrolysis process ( $\text{N}_2$  elimination process) of **EC-1**

**Table S2.**  $OB$  (%),  $\rho$  ( $\text{g}\cdot\text{cm}^{-3}$ ),  $\Delta H_f^\circ(\text{s})$  ( $\text{kcal}\cdot\text{mol}^{-1}$ ),  $D$  ( $\text{km}\cdot\text{s}^{-1}$ ),  $P$  (GPa),  $\Delta V$  ( $\text{\AA}^3$ ), and  $\rho Q_{\max}$  ( $\text{kcal}\cdot\text{cm}^{-3}$ ) of **EC-1**, *trans*-**BIT**, and **RDX**.

	$OB$	$\rho$	$\Delta H_f^\circ(\text{s})$	$D$	$P$	$\Delta V$	$\rho Q_{\max}$
<b>EC-1</b>	-23.18	1.89	36.99	8.851	35.8	47	2.70
<i>Trans</i> - <b>BIT</b> <sup>9</sup>	0	2.06	-95.28	9.473	42.2	72	3.08
<b>RDX</b> <sup>10</sup>	-21.61	1.82	18.9±1.2	8.754	34.7	46	2.71

**Table S3.** Cell parameters predicted with Dreiding force field for **EC-1**

parameters	<i>C2/c</i>	<i>P1</i>	<i>P2<sub>1</sub></i>	<i>P2<sub>1</sub>/c</i>	<i>P2<sub>1</sub>2<sub>1</sub>2<sub>1</sub></i>	<i>Pbca</i>	<i>Pna2<sub>1</sub></i>
<i>Z</i>	8	2	2	4	4	8	4
$\rho(\text{g}\cdot\text{cm}^{-3})$	1.85	1.87	1.86	1.86	1.90	1.87	1.84
$E(\text{kcal}\cdot\text{mol}^{-1}\cdot\text{cell}^{-1})$	43.32	42.69	42.88	42.76	42.16	43.08	43.18
<i>a</i> (Å)	16.72	12.66	6.55	7.90	11.44	7.87	13.41
<i>b</i> (Å)	14.10	7.14	11.01	22.55	6.82	11.02	6.55
<i>c</i> (Å)	12.09	6.46	6.85	7.10	12.40	22.68	11.33
$\alpha$ (°)	90	108.11	90	90	90	90	90
$\beta$ (°)	44.11	117.88	90.83	51.03	90	90	90
$\gamma$ (°)	90	78.71	90	90	90	90	90

**Figure S7.** The most possible crystal packing of **EC-1** predicted by using Dreiding force field.**Figure S8.** The predicted IR spectrum of **EC-1** at the M06-2X/6-31G(d) level.

The IR spectrum was predicted at the M06-2X/6-31G(d) level, with a scale factor of 0.947. For the complexity of vibration modes, only some characteristic vibration modes are assigned here. In **EC-1**, 1795.27  $\text{cm}^{-1}$  belongs to  $\text{NO}_2$  antisymmetric stretching vibration, 1492.50  $\text{cm}^{-1}$  to  $\text{CH}_2$  shear vibration, 1456.49  $\text{cm}^{-1}$  to  $\text{NO}_2$  symmetric stretching vibration, 793.60-949.65  $\text{cm}^{-1}$  to deformation vibration of the molecular skeleton.

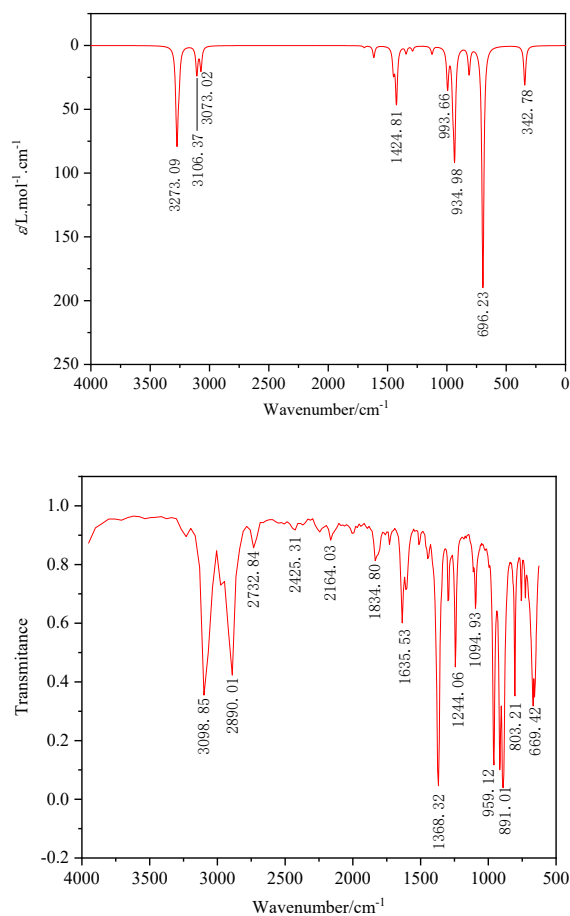


**Figure S9.** The predicted IR spectrum of cyclopentadiene (**0N**) at the M06-2X/6-31G(d) level (up) and its experimental IR spectrum (bottom)

In comparison with the predicted and experimental IR spectra of cyclopentadiene (**0N**), we can see that the IR spectrum of **0N** predicted at the M06-2X/6-31G(d) level was a little bit blue shifted. It suggests that the IR spectrum of **EC-1** predicted at the M06-2X/6-31G(d) level (**Figure S8**) may also a little bit blue shifted.



**The Cartesian coordinates of all involved compounds in the reaction process of EC-1 optimized at the M06-2X/6-31G(d) level**

Frequency calculations ensure that reactants and products do not have any imaginary frequency and transition states (TSs) have only one imaginary frequency.

**Reactant, i.e., 2N-III + TNE**

C	-0.96704300	-0.65953700	0.01561300
C	-0.96728400	0.65928900	-0.01563000
N	1.73479500	0.55303900	-0.45386900
N	1.73497300	-0.55246500	0.45390000
N	-0.93296600	-1.43416100	1.26346900
O	-1.19895900	-0.83002300	2.27779100
O	-0.64479900	-2.60141000	1.14722900
N	-0.96194000	1.53311200	1.17596700
O	0.08626100	1.67070800	1.75170700
O	-2.02877500	2.04972400	1.41166500
N	-0.93357600	1.43392200	-1.26348500
O	-1.19893300	0.82953900	-2.27783700
O	-0.64631400	2.60138800	-1.14725700
N	-0.96141900	-1.53342500	-1.17594700
O	0.08682400	-1.67084200	-1.75162200
O	-2.02813100	-2.05031200	-1.41161200
C	3.92818200	0.00059500	-0.00002400
H	4.57714100	-0.56133800	-0.68271600
H	4.57637000	0.56305800	0.68300300
C	2.94608000	-0.87015000	0.71432400
H	3.17805900	-1.69070200	1.38400900
C	2.94581000	0.87097400	-0.71443400
H	3.17749000	1.69160600	-1.38412800

**TS**

C	0.67242500	0.14869700	0.29718000
C	-0.67605900	0.30376900	0.08288200
N	-0.72903700	-2.22570700	-0.84079700
N	0.60281800	-2.34425800	-0.73950600
N	1.66597900	1.23715800	0.01527700
O	1.65544000	2.11198300	0.84597500
O	2.38403100	1.14029900	-0.95009000
N	-1.17472300	1.49768100	-0.64139900
O	-0.36298400	2.13088000	-1.28746900
O	-2.35876500	1.71957200	-0.55036000
N	-1.72085600	-0.08167700	1.10779600
O	-1.63325700	0.57318500	2.12040100
O	-2.55484100	-0.89244000	0.81106800
N	1.15508100	-0.70341700	1.40027500

O	0.33533100	-1.42789800	1.91553700
O	2.33733800	-0.62249600	1.64826000
C	0.20332300	-0.68252000	-2.29909800
H	0.23114100	-1.19786600	-3.27380900
H	0.33858500	0.38364600	-2.47389400
C	1.18801800	-1.35903800	-1.41252800
H	2.26844000	-1.30065500	-1.46999500
C	-1.02017100	-1.15468300	-1.58362100
H	-2.05657700	-0.94561800	-1.82927300

**Product, i.e., EC-1**

C	-0.78055100	-0.06189500	0.04756600
C	0.76538000	0.08829500	0.13088700
N	0.70288400	-1.99348900	1.38852200
N	-0.52999900	-2.08132300	1.33622900
N	-1.50096500	1.25533500	-0.20196100
O	-1.21699600	1.79378100	-1.24313600
O	-2.28378500	1.61752300	0.64186900
N	1.28525600	1.53904100	0.17338300
O	0.60366600	2.35545300	0.75260900
O	2.38788800	1.70497800	-0.28105500
N	1.53035800	-0.51413100	-1.03417400
O	1.23050000	-0.06946400	-2.11565800
O	2.38107300	-1.32145200	-0.75766700
N	-1.31731200	-0.98619100	-1.05289200
O	-0.61291100	-1.90111400	-1.39923900
O	-2.45802200	-0.76298100	-1.38101000
C	-0.11010700	-0.02157200	2.34710700
H	-0.12321600	-0.46318200	3.34530800
H	-0.20992600	1.06087300	2.40306900
C	-1.11847800	-0.69541400	1.41943200
H	-2.18099100	-0.70125100	1.64645200
C	1.07197600	-0.53673700	1.51647800
H	2.10196000	-0.40098300	1.83889500

**The Cartesian coordinates of all involved compounds in the N<sub>2</sub> elimination process of EC-1 optimized at the M06-2X/6-31G(d) level**

Frequency calculations ensure that reactants and products do not have any imaginary frequency and transition states (TSs) have only one imaginary frequency.

**EC-1**

C	-0.78055100	-0.06189500	0.04756600
C	0.76538000	0.08829500	0.13088700
N	0.70288400	-1.99348900	1.38852200
N	-0.52999900	-2.08132300	1.33622900
N	-1.50096500	1.25533500	-0.20196100
O	-1.21699600	1.79378100	-1.24313600
O	-2.28378500	1.61752300	0.64186900
N	1.28525600	1.53904100	0.17338300
O	0.60366600	2.35545300	0.75260900
O	2.38788800	1.70497800	-0.28105500
N	1.53035800	-0.51413100	-1.03417400
O	1.23050000	-0.06946400	-2.11565800
O	2.38107300	-1.32145200	-0.75766700
N	-1.31731200	-0.98619100	-1.05289200
O	-0.61291100	-1.90111400	-1.39923900
O	-2.45802200	-0.76298100	-1.38101000
C	-0.11010700	-0.02157200	2.34710700
H	-0.12321600	-0.46318200	3.34530800
H	-0.20992600	1.06087300	2.40306900
C	-1.11847800	-0.69541400	1.41943200
H	-2.18099100	-0.70125100	1.64645200
C	1.07197600	-0.53673700	1.51647800
H	2.10196000	-0.40098300	1.83889500

**TS**

C	-0.05138100	-0.78583400	0.20304700
C	-0.04364900	0.78521700	0.15059200
N	2.80555000	0.58327000	0.74124100
N	2.80707400	-0.53422200	0.75954100
N	-1.51385700	-1.31886400	0.42002000
O	-2.15529900	-0.72718100	1.26678300
O	-1.82311800	-2.32251400	-0.15935800
N	-1.48346900	1.35472900	-0.07777000
O	-1.86252200	2.19397900	0.69409200
O	-2.05447700	0.90218000	-1.03986500
N	0.71002600	1.43511100	-1.03506400
O	1.53924900	0.78140800	-1.61417200
O	0.43993300	2.60131400	-1.20146500
N	0.38719000	-1.50870400	-1.07042000

O	1.23025700	-2.36041000	-0.93141600
O	-0.19840100	-1.18960300	-2.07310700
C	0.65743000	0.04870000	2.27872200
H	1.21929800	0.08503600	3.20974100
H	-0.45103000	0.01088400	2.52789400
C	0.68425800	-1.14326800	1.45390900
H	0.70312100	-2.16478700	1.80961500
C	0.58734900	1.21274400	1.42046300
H	0.61199000	2.25087700	1.71759200

**N<sub>2</sub> elimination product**

C	0.53407800	-0.74511500	-0.22465400
C	0.00304000	0.70508800	-0.15773100
N	-4.04856900	0.04824200	-0.50015800
N	-4.33250100	-0.97725200	-0.22624500
N	1.93881900	-0.75095100	-0.86287700
O	2.02014600	-0.07098800	-1.86376400
O	2.78405200	-1.44330900	-0.36404000
N	1.07576800	1.77124400	-0.06360900
O	0.80984300	2.82835000	-0.58462900
O	2.07182400	1.48224700	0.55742200
N	-0.85636000	0.88920700	1.09504800
O	-1.66520900	0.00624600	1.28344200
O	-0.70752800	1.90171500	1.72662400
N	0.70282700	-1.43388900	1.11757500
O	0.56240400	-2.63358200	1.10552900
O	0.99392700	-0.73097500	2.05681400
C	-1.18450200	-0.55927200	-1.77849200
H	-1.92616200	-0.81179900	-2.52811800
H	-0.36292000	1.40234600	-2.16290900
C	-0.41453700	-1.44168600	-1.14855400
H	-0.38345700	-2.51664600	-1.26545000
C	-0.91029400	0.86496800	-1.38342200
H	-1.80973600	1.43837400	-1.14372500

## References

1. M. J. Frisch, G. W. Trucks, H. B. Schlegel, G. E. Suzerain, M. A. Robb, J. J. R. Cheeseman, J. A. Montgomery, T. Vreven, K. N. Kudin, J. C. Burant, J. M. Millam, S. S. Iyengar, J. Tomasi, V. Barone, B. Mennucci, M. Cossi, G. Scalmani, N. Rega, G. Petersson, H. Nakatsuji, M. Hada, M. Ehara, K. Toyota, R. Fukuda, J. Hasegawa, M. Ishida, T. Nakajima, Y. Honda, O. Kitao, H. Nakai, M. Klene, X. Li, J. E. Knox, H. P. Hratchian, J. B. Cross, V. Bakken, C. Adamo, J. Jaramillo, R. Gomperts, R. E. Stratmann, O. Yazyev, A. J. Austin, R. Cammi, C. Pomelli, J. W. Ochterski, P. Y. Ayala, K. Morokuma, G. A. Voth, P. Salvador, J. J. Dannenberg, V. G. Zakrzewski, S. Dapprich, A. D. Daniels, M. C. Strain, O. Farkas, D. K. Malick, A. D. Rabuck, K. Raghavachari, J. B. Foresman, J. V. Ortiz, Q. Cui, A. G. Baboul, S. Clifford, J. Cioslowski, B. Stefanov, G. Liu, A. Liashenko, P. Piskorz, I. Komaromi, R. L. Martin, D. J. Fox, T. Keith, M. A. Al-Laham, C. Y. Peng, A. Nanayakkara, M. Challacombe, P. M. W. Gill, B. Johnson, W. Chen, M. W. Wong, C. Gonzalez and J. A. Pople, *Gaussian 09, Revision A.02*, Wallingford, 2009.
2. P. Politzer, J. Martinez, J. S. Murray, M. C. Concha and A. Toro-Labbe, *Mol. Phys.*, 2009, **107**, 2095-2101.
3. B. M. Rice, S. V. Pai and J. Hare, *Combust. Flame*, 1999, **118**, 445-458.
4. P. Politzer and J. S. Murray, *Propellants Explos. Pyrotech.*, 2016, **41**, 414-425.
5. P. Politzer and J. S. Murray, *J. Mol. Model.*, 2015, **21**, 25.
6. P. Politzer and J. S. Murray, *J. Mol. Model.*, 2015, **21**, 262.
7. S. L. Mayo, B. D. Olafson and W. A. Goddard, *J. Phys. Chem.*, 1990, **94**, 8897-8909.
8. Materials Studio, Version 4.4, Accelry software Inc: San Diego, CA, 2008.
9. J. Yang, X. Gong, H. Mei, T. Li, J. Zhang and M. Gozin, *J. Org. Chem.*, 2018, **83**, 14698-14702.
10. P. Politzer and J. S. Murray, *Cent. Eur. J. Energ. Mater.*, 2011, **8**, 209-220.